Development of bifacial inverted polymer solar cells using a conductivity-controlled transparent PEDOT: PSS and a striped Au electrode on the hole collection side

Development of Bifacial Inverted Polymer Solar Cells using a Conductivity-Controlled Transparent PEDOT:PSS and a Striped Au Electrode on the Hole Collection Side

Takayuki Kuwabara[1,2,*], Shinji Katori[1], Kazuhiro Arima[1], Yoshihiro Omura[1], Takahiro Yamaguchi[1], Tetsuya Taima[1,2,3], and Kohshin Takahashi[1,2,*]

[1]Graduate School of Natural Science and Technology, Kanazawa University, Kakuma-machi, Kanazawa, Ishikawa 920-1192, Japan

[2]Research Center for Sustainable Energy and Technology, Kanazawa University, Kakuma-machi, Kanazawa, Ishikawa 920-1192, Japan

[3]JST-PRESTO, Japan Science and Technology Agency (JST), 4-1-8 Honcho Kawaguchi, Saitama 332-0012, Japan

An inverted bifacial polymer solar cell was developed using a conductivity-controlled transparent PEDOT:PSS as a hole collection layer and a striped Au electrode with a large open aperture ratio (R_{ap}) as a hole collection electrode. We investigated the performance of the device by varying the inter-electrode distance of the striped Au electrode and the sheet resistance of the PEDOT:PSS film. The device using Clevios P (PEDOT:PSS) showed a maximum electric output (P_w) in the R_{ap} range of 50 to 65 %. When alcohol-treated Clevios P (Clevios P+) with a lower electrical resistance was used, the maximum P_w increased by 40 % compared with that of the device using Clevios P. The maximum P_w was obtained in the R_{ap} range of 84 % as the hole collection efficiency of the striped Au electrode improved with the decreased sheet resistance of the PEDOT:PSS.

KEYWORDS: bifacial device, hole collection, inverted polymer solar cells, PEDOT:PSS, striped electrode

*E-mail: tkuwabar@se.kanazawa-u.ac.jp

1. Introduction

Polymer solar cells have attracted worldwide attention as they are low-cost, lightweight, flexible and environmentally friendly[1-8]. They are viable candidates as post-silicon solar cells that can be applied as power generation alternatives on windows[9], plastic sheets[10-12], fibers[13,14] and the insides of rooms. Bifacial solar cells are specially structured solar cells that generate electricity from both sides of the solar cell. They are transparent, have a vertical installation and higher output power. Bifacial polymer solar cells have the potential to act as a power generation system in places that are usually difficult to install such systems. However, reports on bifacial cells have been few, though it is important to encourage their widespread use[15-18].

We have previously studied electron collection layers, such as titanium oxide (TiO_x and TiO_2)[19-21], zinc oxide (ZnO)[22] and zinc sulfide[23], for inverted polymer solar cells. We examined the performance of inverted cells using TiO_x and ZnO prepared by novel chemical-bath-deposition and sol-gel methods, and have developed long-life devices[19,21] as well as flexible devices[11,24]. We have further reported how UV light irradiation affects the photovoltaic characteristics[22,25,26]. Recently we reported that inverted polymer solar cells using ZnO showed a UV light dependence of the device performance that was related to the preparation temperature of the ZnO[26]. This dependence is responsible for forming charge-trapping sites at the ZnO/active layer interface that act as recombination centers for photo-produced charges in the active layer. We also found that for the cell with ZnO prepared by heating at 250 °C, a high power conversion efficiency (PCE) was maintained even under continuous irradiation with simulated sunlight without UV. To develop bifacial inverted polymer solar cells, it is necessary to design the back Au electrode for light irradiation while also allowing for the device function under illumination with light in the non-UV region. UV light is completely absorbed by the active layer under irradiation from the Au side and consequently does not reach the electron collection layer. It is likely that our previous work is only part of the development of these bifacial devices. This current work was done to develop an efficient bifacial

inverted polymer solar cell using a conductivity-controlled transparent PEDOT:PSS as a hole collection layer and a striped Au electrode with a large open aperture ratio as a hole collection electrode. Fig. 1a and b show the schematic device structures of the monofacial and bifacial inverted polymer solar cells. We discuss how the inter-electrode distance of the striped Au electrode and the sheet resistance of the PEDOT:PSS are reflected in the characteristics of the bifacial devices.

2. Experimental Section

Zinc acetylacetonate, acetylacetone, 2-methoxyethanol, regioregular P3HT (average Mn 54,000–75,000), Triton-X 100 and o-dichlorobenzene (o-DCB) were purchased from Sigma-Aldrich Chemical Co., Inc. PCBM was purchased from Frontier Carbon Corporation. Four kinds of PEDOT:PSS dispersions in water (Clevios P, PVPAI4083, PH510, and PHCV4) were purchased from H. C. Starck GmbH, and their PEDOT:PSS ratios were 1:2.5, 1:6, 1:2.5, and 1:2.5 (by weight), respectively. All chemicals were used as received. Glass-ITO substrates (sheet resistance = 10 Ω/sq) and an Au wire were purchased from the Furuuchi Chemical Corporation. The glass-ITO electrodes were cleaned by sonication in 2-propanol, washed in boiling 2-propanol and then dried in air. The fabrication was carried out in air, controlling the relative humidity to less than 35 %. The ZnO film of about 60 nm thickness was deposited on the glass-ITO by the method described in our previous paper[11] and annealed at 250 °C for 1 h on a hot plate. A mixed o-DCB solution of P3HT and PCBM (weight ratio = 5:4) was spin-coated onto the ITO/ZnO, and then the P3HT:PCBM film was solvent-annealed for 40 min in an airtight container. A PEDOT:PSS dispersion in water containing 0.5 wt.% Triton-X 100 was spin-coated onto the PCBM:P3HT layer. The thicknesses of the P3HT:PCBM and PEDOT:PSS films were 200 nm and 190 nm, respectively. To make a typical monofacial device, as illustrated in Fig. 1a, an Au back electrode was vacuum deposited at 2×10^{-5} torr onto the PEDOT:PSS layer with a shadow mask. However, to make a bifacial device, as illustrated in Fig. 1b, an Au back electrode with an inter-electrode distance of 0.19 to 2.88 mm composed of long Au electrodes of about 0.22 mm width was deposited onto the PEDOT:PSS layer using six kinds of slit-like shadow masks. The distance between the Au electrode strips was denoted as W_{int}. Finally, the monofacial and bifacial devices were mechanically protected by laminating with a film (moisture-proof sheet “CELLEL F1550H”, Kureha Extech Co., Ltd.) at 150 °C for 5 min under a reduced atmosphere. The photo-irradiation area was limited to 1 cm^2 by making the ITO electrode of 1 cm width and the Au electrode of 1 cm width cross. This limited area was restricted to

about 1 cm^2 by covering both sides of the front ITO and the back Au with black tape. A photograph of the bifacial devices taken from the Au side is shown in Fig. 2. The photo-irradiation area surrounding the black tape and the slit interval of the Au electrode strips were measured with a microscope (USB Microscope M3, Scalar Corp.). The open aperture ratio of the striped Au electrode, R_{ap}, was obtained by estimating these areas. The I-V curves of the solar cells were measured by linear sweep voltammetry at a scan rate of 5 V min^{-1}, under AM 1.5G simulated sunlight irradiation at an intensity of 100 mW/cm^2 (1 sun). The light source was a solar simulator (XES-502S, SAN-EI Electric Co., Ltd.) calibrated with a standard silicon photovoltaic detector. All electric measurements were performed using an electrochemical analyzer (HZ-5000, Hokuto Denko Corp.). All measurements were carried out under an ambient atmosphere (ca. 25 °C/40–60 %RH). The thickness of the P3HT:PCBM and PEDOT:PSS films were measured by a microfigure measuring instrument (Surfcorder ET200, Kosaka Laboratory Ltd.). Electrical resistance was measured by the one terminal pair network method or the four-poles method, using a precision LCR meter (4284A, Hewlett-Packard Com.) or Ohm tester (3565, Tsuruga Electric Corp.).

3. Results and Discussion

To develop an efficient bifacial solar cell, we need to identify a transparent PEDOT:PSS film that can efficiently collect photo-produced holes on the Au electrode. We first evaluated the performance of monofacial inverted polymer solar cells using five kinds of PEDOT:PSS films with various sheet resistance. The results are summarized in Table I. When the PEDOT:PSS with a sheet resistance of 5×10^4 to 1×10^8 Ω/sq was used as the hole collection layer, there were no great differences in the electric output (P_w). These PEDOT:PSS films included Clevios PVPAI4083, P, P+ and PH510. Clevios P+ represents the Clevios P film after being processed with 2-propanol[27]. It is known that conductivity of PEDOT:PSS enhances by treatment with sugar alcohol[28,29], organic solvent[30-32] and surfactant. However, when Clevios PHCV4 with the lowest sheet resistance was

used as the hole collection layer, the short circuit photocurrent (J_{sc}), the open light voltage (V_{oc}) and fill factor (FF) were lower than those of the other devices, and resulted in the P_w being quite low. This is perhaps because the electron-blocking ability of PEDOT:PSS is low when the electrical resistance is low, and charge recombination may take place easily at the P3HT:PCBM/PEDOT:PSS interface using the PEDOT:PSS with low electrical resistance.

Next, the bifacial devices with the striped Au electrodes at 0.19 mm intervals (Device 1) were fabricated using Clevios PVPAI4083, P, and P+. The P_w was evaluated by irradiating light from both sides of the front ITO and the back Au. We checked that the devices showed photovoltaic properties even when illuminated from the striped back Au electrode. The performance of the bifacial devices is summarized in Table II. The P_w was quite low by the back Au side irradiation compared with the front ITO side irradiation. This is because the Au electrode interrupts the incidence of light and decreases the amount of incident light entering the photoactive layer. When irradiating from the front ITO, the bifacial cells using Clevios P and P+ with lower sheet resistance showed a slightly lower P_w compared with the monofacial cells. However, the P_w of the bifacial cell using Clevios PVPAI4083 with high sheet resistance greatly decreased compared with that of the monofacial cell. This is because the strong electrical resistance in the Clevios PVPAI4083 film prevents lateral motion of the holes. As a result, only the holes near the Au electrode can be collected.

The performance of bifacial inverted polymer cells with various striped Au electrodes using Clevios P and P+ was evaluated to investigate the relation of R_{ap} and P_w. Fig. 3 shows the I-V curves obtained by irradiating the front ITO side of five kinds of devices using Clevios P. The bifacial devices with comparatively narrow slit width (Devices 1 and 2) showed slightly inferior performance compared with the monofacial device, but a significant performance decrement was observed for the bifacial devices with wider slits (Devices 4 and 6). The relations of R_{ap} and P_w for all of the bifacial devices fabricated in this work are shown in Fig. 4. The scale of the W_{int} is attached to the upper horizontal axis to identify the relation between W_{int} and R_{ap}. It was found from the plots ● and ● in

Fig. 4 obtained by irradiating the front ITO side that the P_w of the bifacial devices was lower than that of the monofacial device (gray broken straight line). The P_w of the bifacial devices using Clevios P+ was also higher than that of the bifacial devices using Clevios P although both devices noted that the P_w decreased with the increase in R_{ap}. These results clearly show that the lateral motion of the holes was restricted by the strong electrical resistance of the PEDOT:PSS film. The photo-produced holes cannot be efficiently collected by the striped Au electrodes when PEDOT:PSS with a high electrical resistance is used as the hole collection layer. The plots ○ and ○ in Fig. 4 were obtained by irradiating the striped back Au electrode side. The gray solid straight line corresponds to an ideal P_w that assumes all of the photo-produced holes arriving at the PEDOT:PSS layer are collected by the striped Au electrode. The experimental data plots exist below the line. The R_{ap} of the striped Au electrode showing the maximum P_w was in the range of 55 to 65 % for the bifacial cells using Clevios P with higher electrical resistance, and was in the range of 75 to 85 % for the bifacial cells using Clevios P+ with lower electrical resistance. The maximum P_w (1.61 mW) using Clevios P+ increased by 40 % compared with the maximum achieved (1.13 mW) using Clevios P. It is worth noting that the R_{ap} can be enlarged to about 85 % when the PEDOT:PSS had moderate electrical resistance.

4. Conclusions

A novel method for producing bifacial inverted polymer solar cells was reported using a combination of a striped Au electrode and a resistance-controlled PEDOT:PSS hole collection layer. The photovoltaic characteristics of this device was determined. For the PEDOT:PSS hole collection layer in the bifacial cell, when the PEDOT:PSS with the lowest sheet resistance was used, the device performance was less than that of other devices because of its lower electron-blocking ability. This allowed charge recombination to take place easily at the P3HT:PCBM/PEDOT:PSS interface. However, the P_w of the bifacial cell using PEDOT:PSS with a high sheet resistance decreased

significantly compared with that of the monofacial cell. This is because the strong electrical resistance prevents lateral motion of the holes in the PEDOT:PSS film, showing that only the holes near the Au electrode can be collected. We evaluated the device performance of bifacial inverted polymer cells with various striped Au electrodes using Clevios P and P+. The maximum P_w was seen when the R_{ap} of the striped Au electrode was between 75 to 85 %, which occurred when Clevios P+ was used. We believe that these results regarding bifacial inverted polymer solar cells are valuable, although we do not completely understand the difference in the photovoltaic characteristics by irradiation from both the ITO and Au sides. Detailed investigations on this performance using other evaluation methods are currently in progress.

Acknowledgments

This work was supported by JSPS KAKENHI Grants-in-Aid for Scientific Research (B), for Young Scientists (A), and Exploratory Research. (Grant No. 24350092, 25708029, and 24655205, respectively), Japan.

References

1) L. M. Chen, Z. Hong, G. Li, Y. Yang: Adv. Mater. **21** (2009) 1434.
2) B. Kippelen, J.-L. Bredas: Energy Environ. Sci. **2** (2009) 251.
3) A. W. Hains, Z. Liang, M. A. Woodhouse, B. A. Gregg: Chem. Rev. **110** (2010) 6689.
4) M. Helgesen, R. Sondergaard, F. C. Krebs: J. Mater. Chem. **20** (2010) 36.
5) F. C. Krebs, J. Fyenbo, D. M. Tanenbaum, S. A. Gevorgyan, R. Andriessen, B. van Remoortere, Y. Galagan, M. Jorgensen: Energy Environ. Sci. **4** (2011) 4116.
6) N. Espinosa, M. Hosel, D. Angmo, F. C. Krebs: Energy Environ. Sci. **5** (2012) 5117.
7) P. Kumar, S. Chand: Prog. Photovolt: Res. Appl. **20** (2012) 377.
8) D. Angmo, F. C. Krebs: J. Appl. Polym. Sci. **129** (2013) 1.
9) C.-C. Chen, L. Dou, R. Zhu, C.-H. Chung, T.-B. Song, Y. B. Zheng, S. Hawks, G. Li, P. S. Weiss, Y. Yang: ACS Nano **6** (2012) 7185.
10) L. Yang, T. Zhang, H. Zhou, S. C. Price, B. J. Wiley, W. You: ACS Appl. Mater.

Interfaces **3** (2011) 4075.

11) T. Kuwabara, T. Nakashima, T. Yamaguchi, K. Takahashi: Org. Electron. **13** (2012) 1136.

12) A. Kim, Y. Won, K. Woo, C.-H. Kim, J. Moon: ACS Nano **7** (2013) 1081.

13) J. Liu, M. A. G. Namboothiry, D. L. Carroll: Appl. Phys. Lett. **90** (2007) 133515.

14) D. Liu, M. Zhao, Y. Li, Z. Bian, L. Zhang, Y. Shang, X. Xia, S. Zhang, D. Yun, Z. Liu, A. Cao, C. Huang: ACS Nano **6** (2012) 11027.

15) J. Huang, G. Li, Y. Yang: Adv. Mater. **20** (2008) 415.

16) Y.-Y. Lee, K.-H. Tu, C.-C. Yu, S.-S. Li, J.-Y. Hwang, C.-C. Lin, K.-H. Chen, L.-C. Chen, H.-L. Chen, C.-W. Chen: ACS Nano **5** (2011) 6564.

17) Z. Liu, J. Li, Z.-H. Sun, G. Tai, S.-P. Lau, F. Yan: ACS Nano **6** (2011) 810.

18) H.-W. Lin, Y.-H. Chen, Z.-Y. Huang, C.-W. Chen, L.-Y. Lin, F. Lin, K.-T. Wong: Org. Electron. **13** (2012) 1722.

19) T. Kuwabara, T. Nakayama, K. Uozumi, T. Yamaguchi, K. Takahashi: Sol. Energy Mater. Sol. Cells **92** (2008) 1476.

20) T. Kuwabara, H. Sugiyama, T. Yamaguchi, K. Takahashi: Thin Solid Films **517** (2009) 3766.

21) T. Kuwabara, H. Sugiyama, M. Kuzuba, T. Yamaguchi, K. Takahashi: Org. Electron. **11** (2010) 1136.

22) T. Kuwabara, Y. Kawahara, T. Yamaguchi, K. Takahashi: ACS Appl. Mater. Interfaces **1** (2009) 2107.

23) T. Kuwabara, M. Nakamoto, Y. Kawahara, T. Yamaguchi, K. Takahashi: J. Appl. Phys. **105** (2009) 124513.

24) I. Sasajima, S. Uesaka, T. Kuwabara, T. Yamaguchi, K. Takahashi: Org. Electron. **12** (2011) 113.

25) T. Kuwabara, C. Iwata, T. Yamaguchi, K. Takahashi: ACS Appl. Mater. Interfaces **2** (2010) 2254.

26) T. Kuwabara, C. Tamai, Y. Omura, T. Yamaguchi, T. Taima, K. Takahashi: Org. Electron. **14** (2013) 649.

27) D. Alemu, H.-Y. Wei, K.-C. Ho, C.-W. Chu: Energy Environ. Sci. **5** (2012) 9662.

28) S. K. M. Jönsson, J. Birgerson, X. Crispin, G. Greczynski, W. Osikowicz, A. W. Denier van der Gon, W. R. Salaneck, M. Fahlman: Synth. Met. **139** (2003) 1.

29) L. A. A. Pettersson, S. Ghosh, O. Inganäs: Org. Electron. **3** (2002) 143.

30) Y. Xia, J. Ouyang: ACS Appl. Mater. Interfaces **4** (2012) 4131.

31) I. Cruz-Cruz, M. Reyes-Reyes, M. A. Aguilar-Frutis, A. G. Rodriguez, R. López-Sandoval: Synth. Met. **160** (2010) 1501.

32) Y. H. Kim, C. Sachse, M. L. Machala, C. May, L. Müller-Meskamp, K. Leo: Adv. Funct. Mat. **21** (2011) 1076.

Table I Performance of monofacial inverted polymer solar cells.

PEDOT:PSS	Sheet resistance / 10^4 Ω sq^{-1}	J_{sc} / mA	V_{oc} / V	FF	P_w [a] / mW
PVPAI4083	14700	7.62	0.59	0.60	2.69
Clevios P	15 ± 5	7.67	0.57	0.61	2.67
Clevios P+ [b]	4.5 ± 0.3	7.97	0.59	0.57	2.68
PH510	12 ± 1	7.72	0.56	0.57	2.43
PHCV4	1.6 ± 0.2	7.57	0.51	0.45	1.73

a) Electric output. Because the simulated solar light with the intensity of 100 mW/cm^2 enters into a 1 cm^2 photoactive layer, the P_w is equal to the power conversion efficiency (PCE).

b) Clevios P+ represents the Clevios P film after the addition processing of 2-propanol dropping.

Table II Performance of bifacial inverted polymer solar cells
with a striped Au electrode of 0.19 mm interval (Device 1).

Irradiation side	PEDOT:PSS	Effective Area [a] / cm^2	J_{sc} / mA	V_{oc} / V	FF	P_w [b] / mW	PCE [c] / %
ITO	PVPAI4083	1.0	5.29	0.56	0.52	1.54	1.54
ITO	Clevios P	1.0	7.75	0.55	0.54	2.29	2.29
ITO	Clevios P+	1.0	8.09	0.55	0.58	2.59	2.59
Au	PVPAI4083	0.43	1.38	0.50	0.42	0.29	0.68
Au	Clevios P	0.44	3.24	0.53	0.57	0.98	2.23
Au	Clevios P+	0.43	3.63	0.53	0.59	1.15	2.64

a) The area in which the simulated solar light with an intensity of 100 mW/cm^2 enters into the photoactive layer. This value is equal to the open aperture ratio, R_{ap}.

b) Electric output.

c) The PCE is obtained by dividing the P_w by the effective area.

Figure caption

Fig. 1 Schematic device structures of (a) monofacial and (b) bifacial inverted polymer solar cells.

Fig. 2 Photographs of the bifacial inverted polymer solar cells with different inter-electrode distance (W_{int}) taken from the Au electrode side. The illumination area was restricted to 1 cm^2 by covering with black tape. R_{ap} represents the open aperture ratio.

Fig. 3 Photo I-V curves of monofacial and bifacial inverted polymer solar cells using Clevios P. The photo irradiation was carried out from the ITO side. Refer to Fig. 2 for Devices 1–6.

Fig. 4 Plots of the electric output (P_w) against the open aperture ratio (R_{ap}) of the Au electrode side. ●: When irradiating the devices using Clevios P+ from the ITO side, ●: When irradiating the devices using Clevios P from the ITO side, ○: When irradiating the devices using Clevios P+ from the Au side, ○: When irradiating the devices using Clevios P from the Au side, Gray broken straight line: P_w of the monofacial device when irradiated from the ITO side, Gray solid straight line: ideal P_w assuming all photo-produced holes arriving at the PEDOT:PSS layer are collected by the striped Au electrodes.

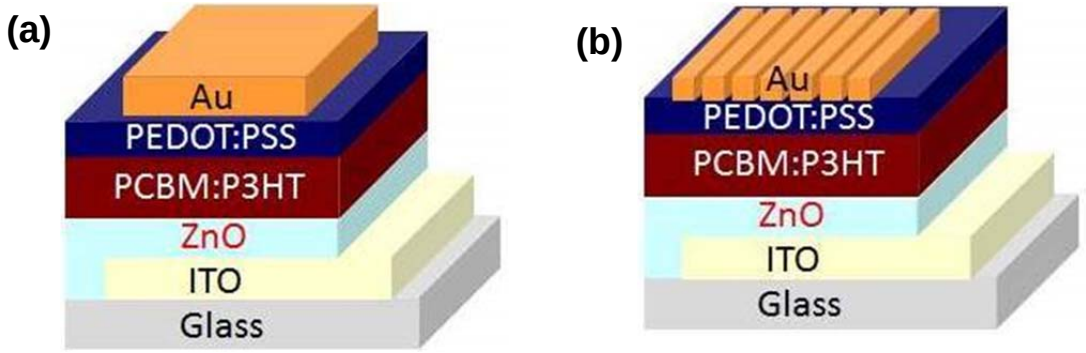

Fig. 1 Kuwabara et al.

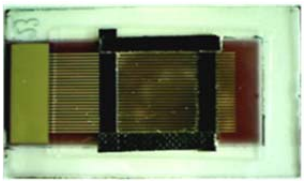

(a) Device 1
W_{int} = 0.19 mm
(R_{ap} = 43 %)

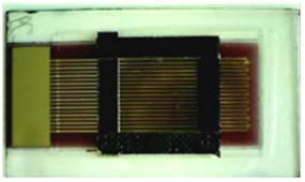

(b) Device 2
W_{int} = 0.27 mm
(R_{ap} = 50 %)

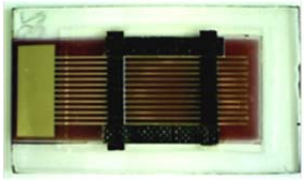

(c) Device 3
W_{int} = 0.49 mm
(R_{ap} = 65 %)

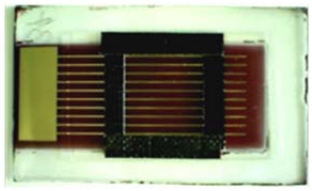

(d) Device 4
W_{int} = 0.87 mm
(R_{ap} = 75 %)

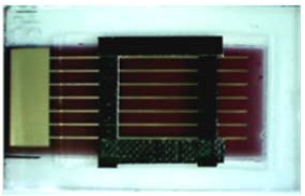

(e) Device 5
W_{int} = 1.42 mm
(R_{ap} = 84 %)

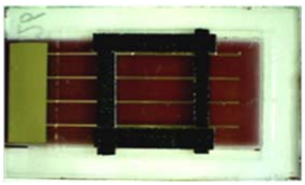

(f) Device 6
Wi_{nt} = 2.82 mm
(R_{ap} = 93 %)

Fig. 2 Kuwabara et al.

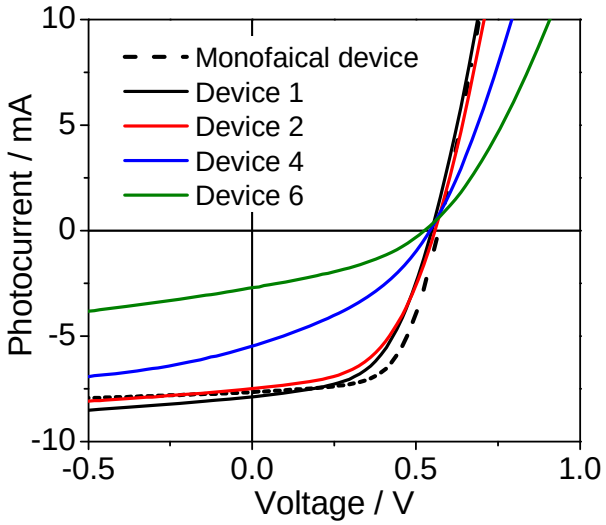

Fig. 3 Kuwabara et al.

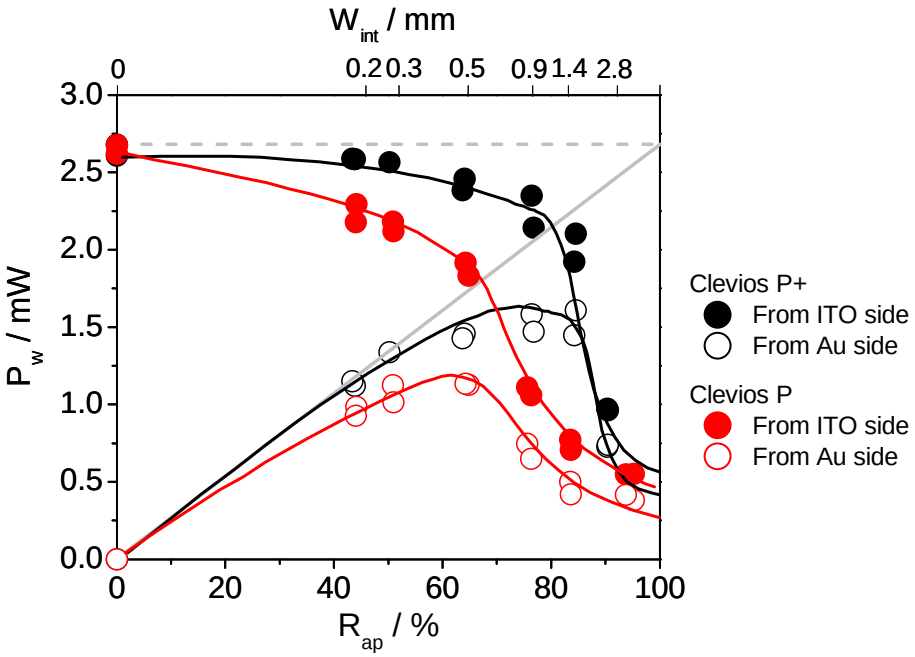

Fig. 4 Kuwabara et al.